

Longitudinal strain with speckle-tracking echocardiography predicts electroanatomic substrate for ventricular tachycardia in nonischemic cardiomyopathy patients



Siddharth J. Trivedi, BSc, BMedSci (Hons), MBBS (Hons), PhD,^{*†}
Timothy Campbell, BSc,^{*‡} Christopher J. Davey, BSc, BE (Hons), PhD,^{*}
Luke Stefani, BBioMedSci,^{*} Liza Thomas, MBBS, PhD,^{*†§1}
Saurabh Kumar, BSc (Med)/MBBS, PhD^{*†‡1}

From the ^{*}Department of Cardiology, Westmead Hospital, Sydney, Australia, [†]Westmead Clinical School, The University of Sydney, Sydney, Australia, [‡]Westmead Applied Research Centre, The University of Sydney, Sydney, Australia, and [§]South Western Sydney Clinical School, University of New South Wales, Sydney, Australia.

BACKGROUND Longitudinal strain (LS) derived from speckle-tracking echocardiography (STE) corresponds to regions of scar in ischemic cardiomyopathy.

OBJECTIVE We investigated if regional LS abnormalities correlate with scar location and scar burden, identified using high-density electroanatomic mapping (EAM) in nonischemic cardiomyopathy (NICM).

METHODS Fifty NICM patients with ventricular tachycardia (VT) underwent echocardiography; multilayer (endocardial, midmyocardial, and epicardial) regional LS and global LS (GLS) were evaluated prior to EAM for detection of low-voltage scar. Patients were divided into 3 groups by EAM left ventricular scar location: (1) anteroseptal (group 1, n = 20); (2) inferolateral (group 2, n = 20); and (3) epicardial scar (group 3; n = 10). We correlated (1) location of scar to regional LS and (2) regional strain and GLS to scar percentage.

RESULTS Regional LS abnormalities correlated with EAM scar in all groups. Segmental impaired LS and low voltage on EAM demonstrated concordance with scar in ~75% or its border zone in 25%

of segments. In groups 1 and 2, endocardial GLS showed a strong linear correlation with endocardial bipolar scar percentage ($r = 0.79, 0.75$ for groups 1 and 2, respectively; $P < .001$), whereas mid-myocardial GLS correlated with unipolar scar percentage ($r = 0.82, 0.78$ for groups 1 and 2, respectively; $P < .001$). In group 3, epicardial regional LS and GLS correlated with epicardial bipolar scar percentage ($r = 0.72, P < .001$).

CONCLUSION Regional abnormalities on LS predict scar location on EAM mapping in patients with NICM. Moreover, global and regional LS correlate with scar percentage. STE could be used as a noninvasive tool for localizing and quantifying scar prior to EAM.

KEYWORDS Ventricular tachycardia; Nonischemic cardiomyopathy; Voltage mapping; Speckle tracking; Strain echocardiography; Global longitudinal strain

(Heart Rhythm 0² 2022;3:176–185) Crown Copyright © 2022 Published by Elsevier Inc. on behalf of Heart Rhythm Society. This is an open access article under the CC BY-NC-ND license (<http://creativecommons.org/licenses/by-nc-nd/4.0/>).

Introduction

Ventricular arrhythmias (VAs) are often related to re-entry around regions of scar in patients with structural heart disease. A key challenge is to accurately identify and localize scar. In advanced disease, scar can be detected visually as regional wall motion abnormality on echocardiography, as areas of

perfusion mismatch on cardiac positron emission tomography (eg, in inflammatory myopathies), or as areas of late gadolinium enhancement by cardiac magnetic resonance imaging (cMRI). Speckle-tracking echocardiography (STE) can quantify myocardial deformation by tracking ultrasonic speckles and can quantify regional and global as well as layer-specific (endocardial, mid-myocardial, and epicardial) longitudinal strain (LS).¹ Abnormalities of myocardial deformation or strain can indicate the presence of scar.²

We recently demonstrated that multilayer strain abnormalities can localize scar and quantify the extent of low-voltage scar detected by electroanatomic mapping (EAM) in

¹Drs Thomas and Kumar are joint senior authors. **Address reprint requests and correspondence:** Associate Professor Saurabh Kumar, Department of Cardiology, Westmead Hospital, Westmead Applied Research Centre, University of Sydney, Hawkesbury Road, Westmead, NSW 2145, Australia. E-mail address: saurabh.kumar@sydney.edu.au.

KEY FINDINGS

- The relationship between noninvasive speckle-tracking echocardiography (STE)-derived strain parameters and invasive electroanatomic mapping (EAM) data in patients with nonischemic cardiomyopathy (NICM) and substrate for ventricular tachycardia (VT) has not been explored. This study demonstrates that global and regional STE parameters correlate with low-voltage scar on EAM in NICM patients.
- Endocardial strain identified bipolar scar, midmyocardial strain identified unipolar scar, and epicardial strain identified epicardial scar, respectively.
- The correlation of global and regional longitudinal strain and scar percentage is linear, and performing noninvasive STE in NICM patients with VT may provide valuable information on scar burden and location, prior to invasive EAM.
- Further studies are required to validate these findings and assess the role of STE in the preprocedural assessment of NICM patients with VT.

ischemic cardiomyopathy (ICM) patients.² As an extension of this work, we hypothesized that regional and layer-specific LS abnormalities may correlate with scar location on high-density EAM in nonischemic cardiomyopathy (NICM) patients, across typical “phenotypes” of anteroseptal and inferolateral endocardial scar³ and epicardial-only scar. Furthermore, we hypothesized that strain could quantify scar burden^{3,4} in this prospective study of NICM patients undergoing STE and high-density EAM prior to ventricular tachycardia (VT) ablation.

Methods

Study population

Fifty consecutive NICM patients with sustained VT who underwent index VT ablation at a tertiary hospital (Westmead Hospital, Sydney, Australia; February 2018 – May 2019) were prospectively recruited. NICM was identified as an absence of significant coronary artery disease and defined according to the criteria of the European Society of Cardiology Working Group on Myocardial and Pericardial Diseases.⁵ Twenty patients, undergoing ablation for other arrhythmias (eg, supraventricular arrhythmias), without scar, were recruited as controls. Patients with a history of nonsustained VT, prior myocardial infarction or obstructive coronary artery disease, congenital heart disease, primary valvular heart disease, hypertrophic cardiomyopathy, or premature ventricular contractions were excluded. Pacing-dependent patients (n = 7) and those with left bundle branch block (n = 4) were excluded; the 50 recruited patients were in sinus or atrial-paced rhythm. Written informed consent was obtained and the study protocol was approved by the Western Sydney Local Health District Human Research Ethics Committee

(HREC Ref: HREC/17/WMEAD/435). The research reported in this paper adhered to the Helsinki Declaration.

Standard echocardiographic assessment

A comprehensive transthoracic echocardiogram was performed prior to their procedure by experienced medical professionals/sonographers, using a commercially available ultrasound machine (Vivid E9; GE Healthcare, Chicago, IL). Images were acquired from the parasternal, apical, and subcostal views; M-mode, 2-dimensional (2D), color, and Doppler images were obtained. Three consecutive beats were acquired at high frame rates (>55 frames/s). Measurements were performed according to the American Society of Echocardiography recommendations⁶ using offline software (EchoPac 201; General Electric, Boston, MA), blinded to patient clinical information.

Speckle-tracking echocardiography

Strain measurements were performed offline, allowing semi-automated analysis (EchoPac 201; General Electric). Global LS (GLS), a measure of left ventricular (LV) longitudinal deformation from apex to base during systole (ie, shortening, hence denoted by negative value), was the average LS from 17 segments from the 3 apical views generated as a “bull’s-eye” map (Supplemental Figure 1). The LV endocardial border was traced in end-systole, with the LV wall subdivided into basal, mid, and apical regions. Peak strain was defined as the peak negative value on the strain curve, including postsystolic peak if present.⁷ Midmyocardial, epicardial, and endocardial peak strain and regional segmental strain were recorded. Segments with poor image quality or inadequate tracking were excluded. An average of 3 measurements was used in the final analysis for strain parameters.

Electrophysiology study, mapping, and radiofrequency ablation

Patients underwent high-density EAM, as previously described.⁸ Intracardiac echocardiography was used for 3-dimensional (3D) biventricular geometry reconstruction (64-element, 5.5–10 Hz; SoundStar, CARTOSOUND module; Biosense Webster, La Jolla, CA). Three-dimensional EAM of the endocardial LV or epicardial LV was performed using the CARTO 3 mapping system (Biosense Webster) using multielectrode mapping catheters (DecaNav or PentaRay; Biosense Webster). An endocardial and/or epicardial 3D shell of chamber geometry was constructed for each ventricle and electrograms recorded during sinus rhythm. A color fill threshold was set at 10 units for all maps. Conventional ventricular peak-to-peak bipolar voltage parameters were used to identify endocardial scar (dense scar: <0.5 millivolts [mV], low voltage: 0.5–1.5 mV, normal >1.5 mV).⁹ Unipolar LV low voltage was defined as electrogram amplitude <8.3 mV¹⁰ and bipolar low voltage <1 mV identified epicardial scar. The annulus was defined as a 1:1 ratio between atrial and ventricular electrograms, and by intracardiac

echocardiography; low-voltage areas within 1 cm of the annulus were excluded from measurements.

LV segmentation and scar analysis

LV voltage maps were manually analyzed as described previously,² with offline analysis performed at 200 mm/s sweep speed. Each electrogram was individually reviewed and annotated. The mitral annulus and aortic valve were excluded from analysis. Scar and low-voltage areas were calculated using the proprietary surface area tool on the EAM system and quantified as (1) endocardial or epicardial surface area (cm²) and (2) proportion of total LV endocardial or epicardial surface area (%). Subsequently, the LV basal and apical landmarks were used to divide the chamber into 17 segments as per the American Heart Association model for myocardial segmentation and similar to the segmentation obtained from the STE bull's-eye map.⁶ The scar area in each segment was measured and, using the LV surface area for that segment, the scar percentage for that segment was determined. For epicardial map analysis, the septal segments were excluded, as there were no adjacent epicardial surfaces to correlate with. As a result, only the remaining segments were analyzed. Only the scar areas overlying the LV epicardium were analyzed.

For correlation between scar location on strain imaging and EAM, 3D EAM segmental data were converted into a 2D, 17-segment "bull's-eye" map similar to the strain map using in-house custom-designed MATLAB software (Mathworks, Natick, MA; [Supplemental Methods](#)). The 17 segments on the 2D "bull's-eye" EAM were correlated with regions of impaired LS on the strain maps using side-by-side comparisons. The two were determined as correlated if the abnormal LS region was located in the same segment as scar or within 1 segment of the scar map region (scar border zone; Graphical Abstract).

Reproducibility

Interobserver and intraobserver reproducibility of GLS (S.J.T., L.S.) and bipolar and unipolar scar (S.J.T., T.C.) on EAM were performed in 15 randomly selected patients by 2 experienced analysts, blinded to each other's measurements and to patient's clinical details.

Subgroups for correlation between STE indices and EAM

We defined 3 subgroups of patients to evaluate correlation between STE and scar pattern on high-density EAM: group 1: isolated anteroseptal scar (n = 20); group 2: isolated inferolateral scar (n = 20); and group 3: LV epicardial scar (n = 10).

Statistical analysis

Continuous variables are presented as mean \pm standard deviation or median (interquartile range [IQR]); categorical variables are summarized using frequencies and percentages. The Pearson rank correlation test was used to assess possible cor-

Table 1 Baseline characteristics

Characteristic	NICM patients undergoing EAM and VT ablation (n = 50)	Controls undergoing EAM (n = 20)
Age (years)	59 \pm 14 years	50 \pm 13
Male	38 (75)	11 (55)
Clinical characteristics		
Hypertension	21 (42)	8 (40)
Diabetes mellitus	9 (18)	2 (10)
Dyslipidemia	16 (32)	6 (30)
Chronic kidney disease	3 (5)	0
History of atrial fibrillation	6 (12)	0
NYHA class III/IV	17 (33)	0
ICD	44 (88)	0
Medical therapy		
Beta-blockers	35 (70)	15 (75)
ACEI/ARB	20 (40)	7 (35)
Spironolactone	8 (16)	0
Furosemide	20 (40)	0
Amiodarone	33 (66)	0
Lignocaine	8 (15)	0
Mexiletine	2 (3)	0
cMRI preprocedure	9 (18)	0
Underlying		
cardiomyopathy		
Idiopathic dilated	40 (80)	0
Arrhythmogenic cardiomyopathy	5 (9)	0
Cardiac sarcoidosis	4 (8)	0
Congenital	1 (1)	0
Scar subtype		
Anteroseptal	20 (40)	0
Inferolateral	20 (40)	0
LV epicardial	10 (20)	0

Values are presented as mean \pm SD or as n (%).

ACEI = angiotensin-converting enzyme inhibitor; ARB = angiotensin receptor blocker; cMRI = cardiac magnetic resonance imaging; EAM = electroanatomic mapping; ICD = implantable cardioverter-defibrillator; LV = left ventricular; NICM = nonischemic cardiomyopathy; VT = ventricular tachycardia.

relations. EAM and echocardiographic parameters among the 3 different groups were analyzed using 1-way ANOVA. Differences were considered significant with a 2-tailed *P* value of $<.05$. Inter- and intraobserver reproducibility are reported as coefficients of repeatability. Statistical analysis was performed using commercially available software (SPSS software 22.0; SPSS Inc, Chicago, IL).

Results

Baseline characteristics

Fifty NICM patients who underwent VT ablation (mean age 59 \pm 14 years; 75% male) and 20 controls who underwent EAM and STE strain evaluation (mean age 50 \pm 13 years; 55% male) were included ([Table 1](#)). Echocardiography was performed 1.9 \pm 1 days prior to EAM. In patients with cMRI (n = 9, 18%), this was performed 21 \pm 12 days prior to EAM.

Table 2 Electroanatomic mapping parameters in nonischemic cardiomyopathy patients and controls

	LV isolated anteroseptal scar (group 1, n = 20)	LV isolated inferolateral scar (group 2, n = 20)	LV epicardial scar (group 3, n = 10)	Controls undergoing EAM (n = 20)	P value (1-way ANOVA) [§]
Total points (n)	963 (544–1986)	1064 (705–2022)	1954 (1840–2143)	775 (521–1010)	<.001
Chamber volume (mL)	196 (176–205)	207 (171–211)	-	144 (105–172)	.078
Chamber surface area (cm ²)	176 (161–196)	181 (166–192)	162 (143–176) [†]	161 (145–178)	.432
Total bipolar scar area <1.5 mV (cm ²)	45 (31–59)	47 (29–63)	49 (38–56) [‡]	0	.137
Bipolar scar area as percentage of chamber total surface area (%)	20 (17–40)	21 (16–42)	27 (20–46)	0	.063
Total unipolar scar area <8.3 mV (cm ²)	56 (46–70)	54 (43–66)	-	0	.273
Unipolar scar area as percentage of chamber total surface area (%)	30 (26–46)	32 (24–46)	-	0	.162

Values are presented as mean ± SD, or median (interquartile range).

EAM = electroanatomic mapping; LV = left ventricular.

[†]Surface area of analyzed segments only.

[‡]Scar area overlying epicardial LV only.

[§]Excludes control group.

Electroanatomic mapping data

A median of 963 (IQR 544–1986) points were collected from LV EAM for group 1, 1064 (IQR 705–2022) for group 2, and 1954 (IQR 1840–2143) for group 3 (Table 2), with no significant differences in chamber volume, surface area, bipolar scar, or unipolar scar among the groups.

Echocardiographic data

There were no differences between the groups for LV size and function parameters (Table 3). Using a 17-segment model, 740 segments were analyzed, and 110 segments were excluded owing to poor image quality and inadequate tracking. Strain in all 3 LV layers demonstrated marked impairment in all groups.

Correlation between strain and voltage data

All 20 controls demonstrated normal multilayer GLS: endocardial GLS -25.3% ± 2.2%, midmyocardial GLS -23.1% ± 2.3%, epicardial GLS -21.0% ± 1.9%. Mean bipolar (5.4 ± 2.0 mV) and unipolar voltage (19.0 ± 5.7 mV) on EAM were also normal in controls. The Pearson correlation between GLS strain indices and global bipolar and unipolar percentage scar are presented in Table 4. When endocardial bipolar scar percentage (groups 1 and 2, n = 40) was evaluated as tertiles (<15% scar, 15%–25% scar, and >25% scar), corresponding endocardial GLS values were -13.4% ± 0.9%, -12.8% ± 1.3%, and -10.7% ± 1.5%, respectively.

Group 1 (anteroseptal scar)

NICM patients with anteroseptal scar (group 1) demonstrated a linear correlation between bipolar and unipolar scar percentage and layer-specific strain indices. Bipolar scar percentage correlated best with endocardial GLS ($r = 0.79$; $P < .001$; Figure 1A), with lower correlations with midmyocardial ($r = 0.77$; $P < .001$) and epicardial GLS ($r = 0.75$;

$P < .001$). Unipolar scar percentage correlated best with midmyocardial GLS ($r = 0.82$; $P < .001$; Figure 1B).

The correlation between segmental LS and bipolar/unipolar scar and mean voltage in the 17 LV segments for group 1 patients is shown in Supplemental Table 1, with good correlation between bipolar voltage and endocardial LS, and between unipolar voltage and midmyocardial LS. Figure 2A illustrates the linear correlation between segmental endocardial LS and segmental endocardial bipolar scar percentage in the 17 LV segments ($r = 0.72$ – 0.82 , $P < .001$).

Figure 3 demonstrates a case example of an NICM patient with anteroseptal scar demonstrating strong regional correlation between the endocardial strain abnormalities that match bipolar scar regions. Similarly, midmyocardial and epicardial strain abnormalities match the unipolar scar regions.

Using a regional LS value of -16% or worse,⁶ the number of segments with impaired endocardial LS for each patient was 7 ± 1 . Using mean voltage <1.5 mV for endocardial bipolar scar, the number of segments with bipolar scar for each patient was 6 ± 1 . Using these cut-off values to identify abnormal segments in 20 patients, endocardial LS and endocardial bipolar voltage were matched in 76% of segments. For the remaining 24%, the segment with impaired endocardial LS was adjacent to that with low bipolar endocardial voltage.

Using mean voltage <8.3 mV for unipolar scar, the number of segments with low endocardial unipolar voltage for patients was 7 ± 1 . Segmental matching for impaired epicardial LS and abnormal endocardial unipolar voltage demonstrated concordance in 70% of segments. In the remaining 30% of segments, impaired endocardial LS was seen in an adjacent segment.

Group 2 (inferolateral scar)

Bipolar scar percentage correlated best with endocardial GLS ($r = 0.75$; $P < .001$), whereas unipolar scar percentage

Table 3 Echocardiographic parameters in nonischemic cardiomyopathy patients and controls undergoing left ventricular electroanatomic mapping

LV echocardiographic variable	LV isolated anteroseptal scar (group 1, n = 20)	LV isolated inferolateral scar (group 2, n = 20)	LV epicardial scar (group 3, n = 10)	Controls undergoing EAM (n = 20)	P value (1-way ANOVA) [†]
LVEDVi (mL/m ²)	98 ± 29	102 ± 31	100 ± 28	51 ± 13	.074
LVEF (%)	44 ± 16	40 ± 14	40 ± 15	60 ± 5	.142
LAVi (mL/m ²)	56 ± 29	55 ± 31	56 ± 30	27 ± 8	.352
LV strain parameters					
Endocardial longitudinal strain (%)	-11.9 ± 3.6	-11.8 ± 3.7	-11.7 ± 3.7	-25.3 ± 2.2	.116
Midmyocardial longitudinal strain (%)	-10.5 ± 3.1	-10.5 ± 3.2	-10.2 ± 2.9	-23.1 ± 2.3	.214
Epicardial longitudinal strain (%)	-9.2 ± 2.7	-9.0 ± 2.9	-9.5 ± 3.1	-21.0 ± 1.9	.187

Values are presented as mean ± SD.

EAM = electroanatomic mapping; LAVi = left atrial volume indexed; LV = left ventricular; LVEDVi = left ventricular end diastolic volume indexed; LVEF = left ventricular ejection fraction.

[†]Excludes control group.

correlated best with midmyocardial GLS ($r = 0.78$; $P < .001$). Regional correlations are presented in [Supplemental Table 2](#). [Figure 2B](#) illustrates the linear correlation between segmental endocardial LS and segmental endocardial bipolar scar percentage in the 17 LV segments ($r = 0.72$ – 0.80 , $P < .001$).

A patient with inferolateral scar and correlation with STE indices is presented in [Figure 4](#), demonstrating strong regional correlation between endocardial strain and bipolar scar regions. Similarly, midmyocardial and epicardial strain abnormalities match the unipolar scar regions.

Endocardial LS and endocardial bipolar voltage matched in 73% of segments; the remaining 27% of segments with impaired endocardial LS were adjacent to segments with low bipolar endocardial voltage.

Similarly, segmental matching for impaired epicardial LS and abnormal unipolar voltage demonstrated concordance in 72% of segments, with the remaining 28% being adjacent segments.

Group 3 (LV epicardial scar)

In the 10 patients with LV epicardial EAM, epicardial GLS correlated with epicardial bipolar scar percentage ($r = 0.72$, $P < .001$). Segmental epicardial strain and epicardial bipolar scar also demonstrated modest correlation

([Supplemental Table 3](#)). [Figure 5](#) presents a case example of an NICM patient with epicardial scar demonstrating good correlation between epicardial strain and epicardial scar.

Reproducibility

Interobserver (S.J.T. and L.S.) and intraobserver (S.J.T.) coefficients of repeatability for GLS were 2.6 and 1.7, respectively, and for regional strain were 2.2 and 1.4, respectively. Interobserver (S.J.T. and T.C.) and intraobserver (S.J.T.) coefficients of repeatability for bipolar scar were 5.6 and 6.6, respectively, and for unipolar scar were 5.4 and 6.2, respectively.

Discussion

This is the first study to comprehensively evaluate the relationship between global and segmental STE strain with invasive high-density EAM in NICM patients with VT. We demonstrate the following key findings: (1) Regional LS abnormalities localized low-voltage bipolar scar in NICM patients; abnormal endocardial strain correlated with regions of endocardial bipolar scar, abnormal midmyocardial strain correlated with regions of endocardial unipolar scar, and abnormal epicardial strain correlated with regions of epicardial scar. (2) LS was able to quantify scar burden, with strong

Table 4 Correlation between scar percentage and strain parameters

Strain parameter	LV isolated anteroseptal scar (group 1, n = 20)				LV isolated inferolateral scar (group 2, n = 20)				LV epicardial scar (group 3, n = 10)	
	Bipolar		Unipolar		Bipolar		Unipolar		Bipolar	
	r	P	r	P	R	P	r	P	r	P
Endocardial GLS	0.79	<.001	0.81	<.001	0.75	<.001	0.72	<.001	0.64	.04
Midmyocardial GLS	0.77	<.001	0.82	<.001	0.69	.001	0.78	<.001	0.66	.03
Epicardial GLS	0.75	<.001	0.79	<.001	0.59	.006	0.76	<.001	0.72	<.001

GLS = global longitudinal strain; LV = left ventricular.

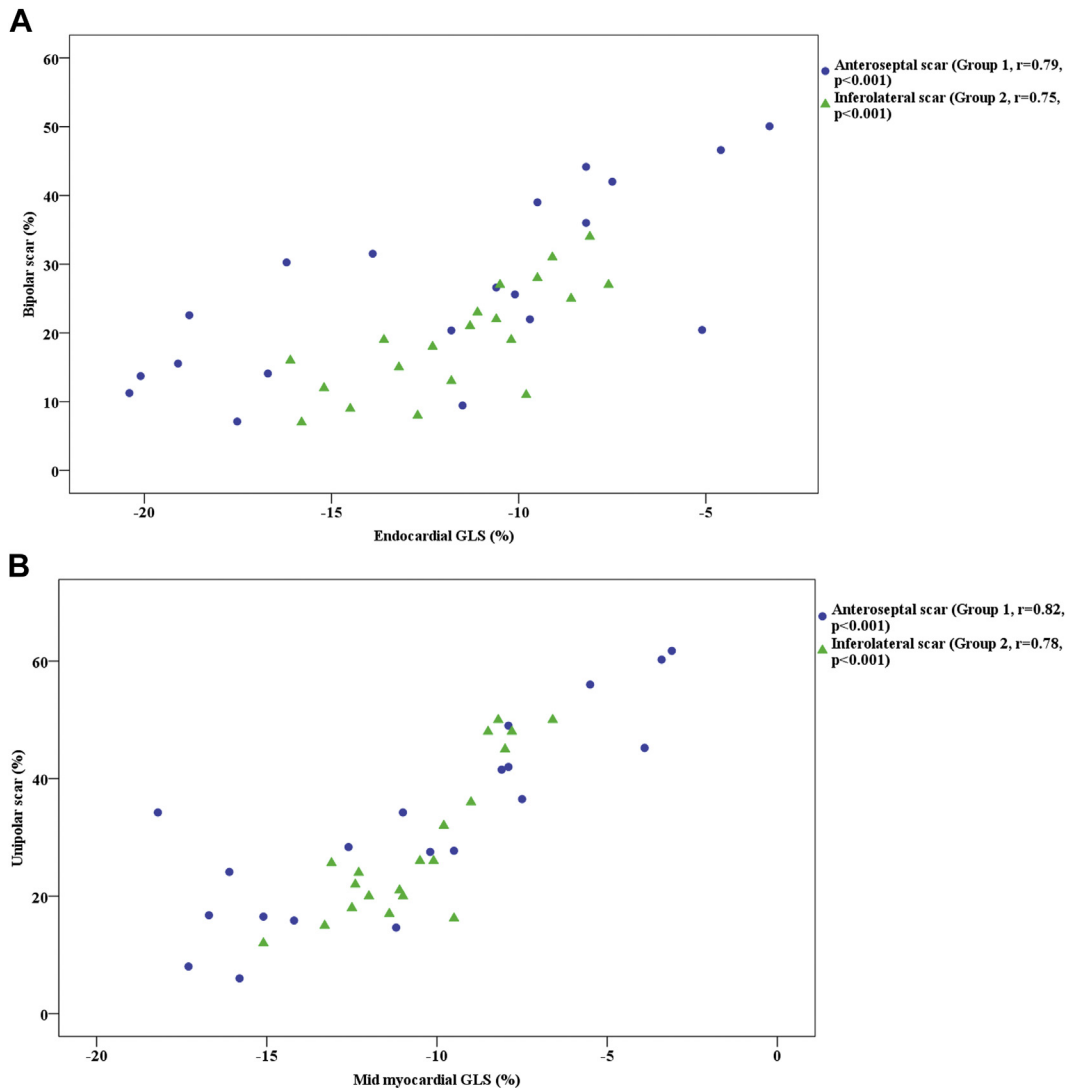


Figure 1 Correlation between electroanatomic mapping scar and speckle-tracking echocardiography strain parameters in nonischemic cardiomyopathy patients. **A:** Correlation between bipolar scar (%) and endocardial global longitudinal strain (GLS; %). **B:** Correlation between unipolar scar (%) and midmyocardial GLS (%).

linear correlation between low-voltage bipolar and unipolar scar percentage with endocardial and midmyocardial LS, respectively.

We extend previous observations that regional and global STE abnormalities can predict scar burden and location in ICM, to patients with NICM.² This noninvasive detection of scar may aid in preemptive “scar” mapping prior to catheter ablation and assist in risk stratification in NICM by identification of arrhythmogenic substrate.

VT in patients with NICM

The majority of VTs in NICM patients are due to scar-mediated re-entry in and around regions of scar.¹¹ The arrhythmia is often precipitated by the interplay between areas of interstitial fibrosis within adjacent areas of healthy myocardium.¹² Crucially, these circuits may

span all 3 myocardial layers in a 3D manner.¹³ The impaired myocardial deformation seen across all myocardial layers in our study—endocardial, midmyocardial, and epicardial—illustrates this concept of profound transmural myocardial alterations.

Scar subtypes in NICM

Two discrete phenotypes based on LV scar regions are recognized in NICM patients—anteroseptal and inferolateral.^{3,4,14} Anteroseptal scar typically involves the basal anteroseptum, periaortic LV, aortomitral continuity, aortic cusps, and right ventricular septum. Often the scar extends intramurally, and epicardial mapping and ablation is of limited value as the right ventricular outflow tract overlies the area superiorly, and fat and coronary arteries are present in the basal region. Our study showed that in this group, endocardial and

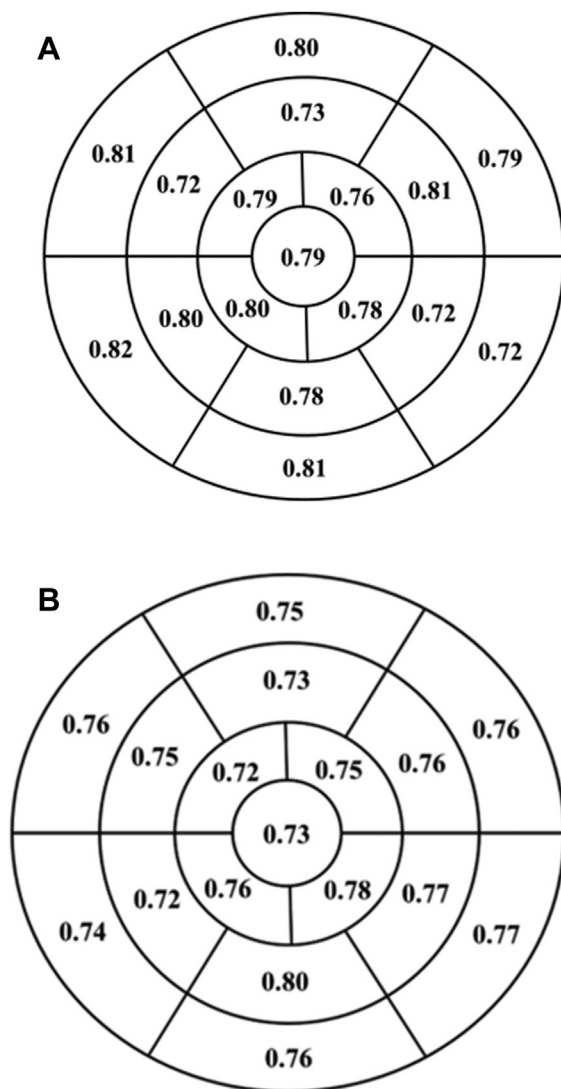


Figure 2 Correlation between segmental endocardial strain and segmental bipolar scar percentage in each left ventricular (LV) segment in patients with anteroseptal scar (group 1, panel A) and inferolateral scar (group 2, panel B). **A:** Correlation between bipolar scar percentage and endocardial longitudinal strain (LS) within LV segments for patients with anteroseptal scar (n = 20). **B:** Correlation between bipolar scar percentage and endocardial LS within LV segments for patients with inferolateral scar (n = 20).

midmyocardial GLS have the strongest correlation with bipolar and unipolar scar, respectively.

In contrast, inferolateral scar can be predominantly epicardial. Midmyocardial strain demonstrated better correlation with unipolar than with bipolar scar in this group of patients. Unipolar recordings represent far-field signals generated by depolarization of tissue remote from the recording electrode,¹⁵ and hence more accurately reflect this midmyocardial/epicardial substrate than bipolar voltage, which records depolarization immediately beneath the recording electrode. Lastly, NICM may have only epicardial scar. In our study, epicardial strain correlated with epicardial scar location and modestly with epicardial scar percentage.

Speckle-tracking strain echocardiography in the assessment of substrate in patients with NICM

STE quantifies myocardial deformation and global and regional LS and can identify fibrosis or scar.¹ While substantial literature demonstrates utility of STE indices for detecting subclinical myocardial dysfunction, there is a paucity of reports that have examined if STE can identify fibrosis and scar localization determined by EAM.² Low-voltage scar by EAM correlates with scar on histopathology.¹⁶ Our study confirms that strain predicts both the regionality and topography of scar seen on EAM in NICM patients.

Previous studies have suggested that LV regions with scar exhibit electromechanical uncoupling.¹⁷ In our study, regional strain demonstrated a good correlation with regional voltage/scar indices, illustrating the utility of strain in localization of fibrosis, that could be used as a surrogate for scar identification and localization.

Finally, strain analysis by semi-automated image processing provides an objective and quantitative marker of both global and segmental contractile function with higher reproducibility of measurement, compared to subjective visual assessment.¹ During EAM, LV contractile function can be assessed intraprocedurally with intracardiac echocardiography; however, this also provides a qualitative rather than quantitative assessment of scarred myocardium.¹⁸

Limitations

This was a single-center study with a modest sample size. However, patients underwent meticulous echocardiographic assessment and high-density voltage maps. Investigators performing STE measurements were blinded to EAM measurements and vice versa. This study was hypothesis generating, and findings require validation.

We recognize that STE has some limitations. The 2D image quality and frame rates remain a crucial determinant of strain assessment.¹⁹ In addition, there are vendor-specific differences and variations in software algorithms; hence cross-platform values are not interchangeable for serial follow-up.²⁰ There has been a call for standardization of STE strain analysis by international societies, minimizing these differences.⁷ In this study, all echocardiograms were performed using single-vendor equipment and software.

Finally, cMRI could not be performed in all patients for several reasons, including the acuity of the patient's presentation, retained defibrillator and/or pacing leads, patient claustrophobia, and renal disease prohibiting use of gadolinium contrast. Only 9 of the patients underwent cMRI; a representative example of 1 of the 9 patients who underwent cMRI, together with EAM and strain images, has been included as an example (Supplemental Figure 2). In addition, epicardial mapping was not performed on all patients, as this was not clinically indicated.

Conclusion

Regional strain abnormalities correlate with regional scar identified on EAM across a variety of NICM scar

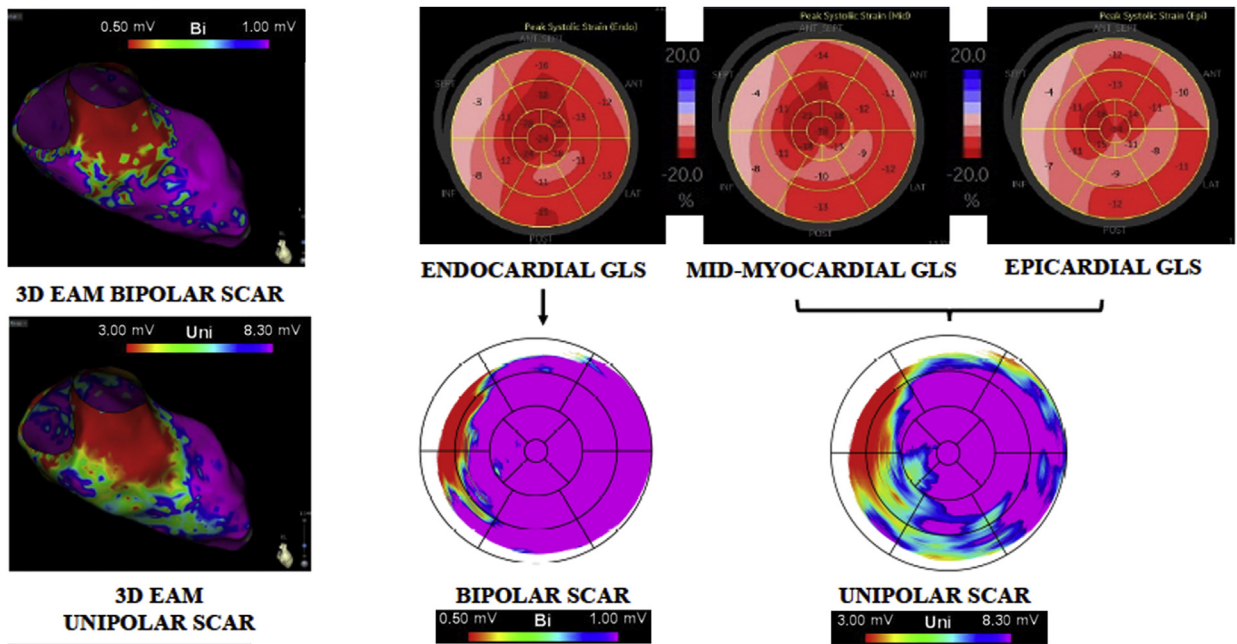


Figure 3 Example of a patient with nonischemic cardiomyopathy (NICM) and anteroapical scar with layer-specific speckle-tracking echocardiography (STE) parameters and bipolar and unipolar scar burden on electroanatomic mapping (EAM). STE and EAM in a 65-year-old man with NICM and ventricular tachycardia from an anteroapical scar. Left upper panel: Three-dimensional (3D) EAM demonstrating bipolar scar. Left lower panel: 3D EAM demonstrating unipolar scar. Right upper panel: Regional endocardial longitudinal strain demonstrating impaired strain in anterior and anteroapical segments (left), midmyocardial global longitudinal strain (GLS; middle), and epicardial GLS (right). Right lower panel: Bipolar scar on EAM demonstrating anterior and anteroapical scar (left), and unipolar scar on EAM (right) demonstrating a larger region of midmyocardial involvement. Low-voltage bipolar areas (<0.5 mV) are in red, healthy bipolar areas (>1.5 mV) are in purple, and colors in between are border zone (0.5–1.5 mV). Low-voltage unipolar areas (<3 mV) are in red, healthy unipolar areas (>8.3 mV) are in purple, and colors in between are border zone (3–8.3 mV).

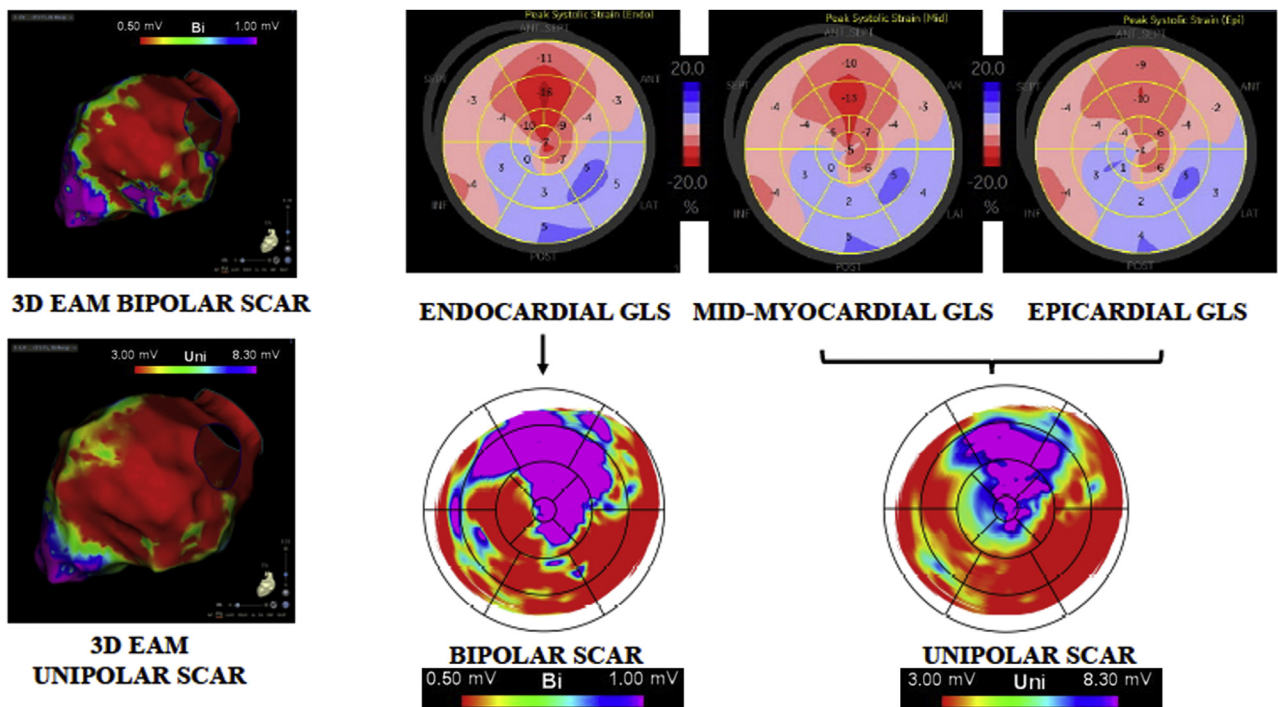


Figure 4 Example of a nonischemic cardiomyopathy (NICM) patient with inferolateral scar with layer-specific speckle-tracking echocardiography (STE) parameters and bipolar and unipolar scar burden on electroanatomic mapping (EAM). STE and EAM parameters in a 68-year-old woman with NICM and an inferolateral scar. Left upper panel: Three-dimensional (3D) EAM demonstrating bipolar scar. Left lower panel: 3D EAM demonstrating unipolar scar. Right upper panel: Endocardial global longitudinal strain (GLS) demonstrating impaired strain in inferolateral segments (left), midmyocardial GLS (middle), and epicardial GLS (right). Right lower panel: Bipolar scar on EAM demonstrating an extensive inferolateral scar (left) and unipolar scar on EAM (right).

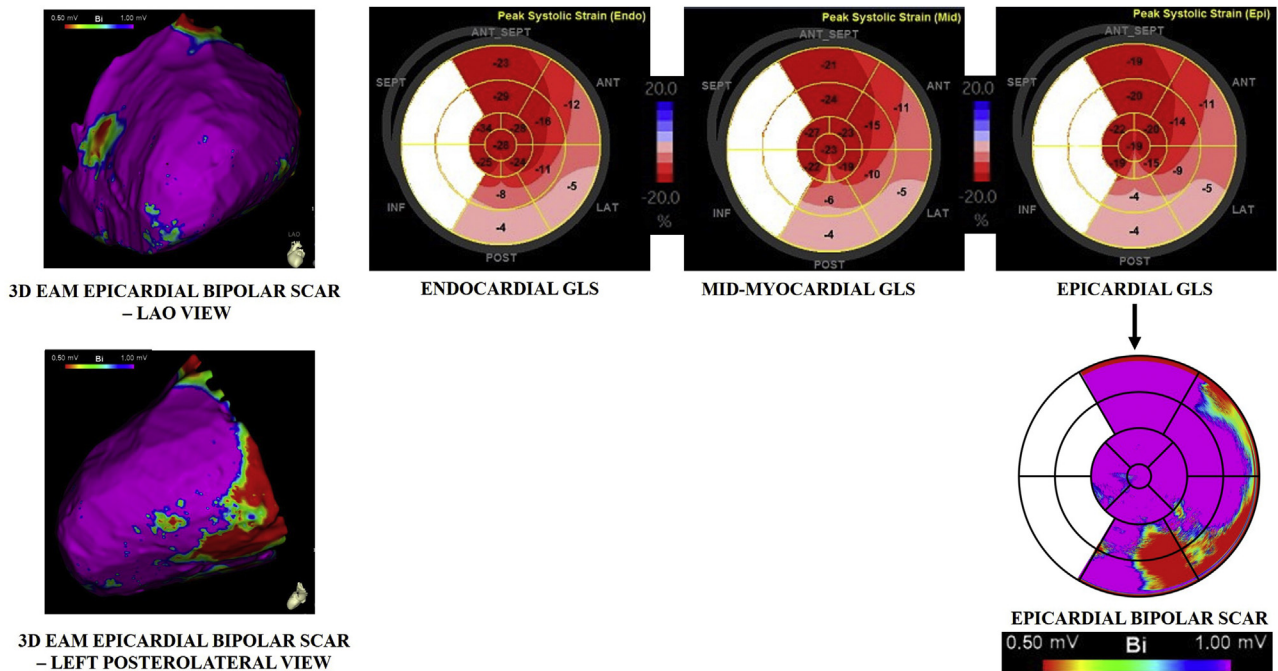


Figure 5 Example of a nonischemic cardiomyopathy (NICM) patient with epicardial scar with layer-specific speckle-tracking echocardiography (STE) parameters and scar burden on epicardial electroanatomic mapping (EAM). STE and EAM parameters in a 60-year-old man with NICM and epicardial scar. Left upper panel: Three-dimensional (3D) EAM demonstrating bipolar scar in the left anterior oblique view. Left lower panel: 3D EAM demonstrating bipolar scar in the left posterolateral view. Right upper panel: Endocardial global longitudinal strain (GLS; left), midmyocardial GLS (middle), and epicardial GLS (right). Right lower panel: Epicardial bipolar scar. The septal segments were excluded from analysis, as there were no adjacent epicardial surfaces with which to correlate.

phenotypes. Endocardial strain identified bipolar scar, midmyocardial strain identified unipolar scar, and epicardial strain identified epicardial scar directly. The correlation of regional and global LS and scar percentage is linear, suggesting that scar burden may be quantified using noninvasive STE analysis. Further validation of these findings is required to confirm the role of STE in the preprocedural assessment of NICM patients with VT.

Funding Sources: S.J.T. has been supported by the Cardiac Society of Australia and New Zealand Research Scholarship (RS2/18) and the National Health and Medical Research Council Postgraduate Scholarship (1168854). This study was supported in part by the Westmead Hospital Charitable Trust grant and the Sylvia and Charles Viertel Charitable Foundation, Clinical Investigator Project Grant awarded to S.K. S.K. is a recipient of the NSW Health Early-Mid Career Fellowship.

Disclosures: The authors have no conflicts to disclose.

Authorship: All authors attest they meet the current ICMJE criteria for authorship.

Patient Consent: Written informed consent was obtained.

Ethics Statement: The study protocol was approved by the Western Sydney Local Health District Human Research Ethics Committee (HREC Ref: HREC/17/WMEAD/435). The research reported in this paper adhered to the Helsinki Declaration.

Appendix Supplementary data

Supplementary data associated with this article can be found in the online version at <https://doi.org/10.1016/j.hroo.2022.02.002>.

References

1. Trivedi SJ, Altman M, Stanton T, Thomas L. Echocardiographic strain in clinical practice. *Heart Lung Circ* 2019;28:1320–1330.
2. Trivedi SJ, Campbell T, Stefani LD, Thomas L, Kumar S. Strain by speckle tracking echocardiography correlates with electroanatomic scar location and burden in ischaemic cardiomyopathy. *Eur Heart J Cardiovasc Imaging* 2021; 22:855–865.
3. Oloriz T, Silberbauer J, Maccabelli G, et al. Catheter ablation of ventricular arrhythmia in nonischemic cardiomyopathy: anteroapical versus inferolateral scar sub-types. *Circ Arrhythm Electrophysiol* 2014;7:414–423.
4. Piers SR, Tao Q, van Huls van Taxis CF, Schalij MJ, van der Geest RJ, Zeppenfeld K. Contrast-enhanced MRI-derived scar patterns and associated ventricular tachycardias in nonischemic cardiomyopathy: implications for the ablation strategy. *Circ Arrhythm Electrophysiol* 2013;6:875–883.
5. Elliott P, Andersson B, Arbustini E, et al. Classification of the cardiomyopathies: a position statement from the European Society of Cardiology working group on myocardial and pericardial diseases. *Eur Heart J* 2007;29:270–276.
6. Lang RM, Badano LP, Mor-Avi V, et al. Recommendations for cardiac chamber quantification by echocardiography in adults: an update from the American Society of Echocardiography and the European Association of Cardiovascular Imaging. *Eur Heart J Cardiovasc Imaging* 2015;16:233–271.
7. Voigt J-U, Pedrizzetti G, Lysyansky P, et al. Definitions for a common standard for 2D speckle tracking echocardiography: consensus document of the EACVI/ASE/Industry Task Force to standardize deformation imaging. *Eur Heart J Cardiovasc Imaging* 2014;16:1–11.
8. Anderson RD, Lee G, Trivic I, et al. Focal ventricular tachycardias in structural heart disease: prevalence, characteristics, and clinical outcomes after catheter ablation. *JACC Clin Electrophysiol* 2020;6:56–69.
9. Marchlinski FE, Callans DJ, Gottlieb CD, Zado E. Linear ablation lesions for control of unmappable ventricular tachycardia in patients with ischemic and nonischemic cardiomyopathy. *Circulation* 2000;101:1288–1296.
10. Hutchinson MD, Gerstenfeld EP, Desjardins B, et al. Endocardial unipolar voltage mapping to detect epicardial ventricular tachycardia substrate in patients with nonischemic left ventricular cardiomyopathy. *Circ Arrhythm Electrophysiol* 2011;4:49–55.
11. Hsia HH, Callans DJ, Marchlinski FE. Characterization of endocardial electrophysiological substrate in patients with nonischemic cardiomyopathy and monomorphic ventricular tachycardia. *Circulation* 2003; 108:704–710.

12. de Bakker JM, van Capelle FJ, Janse MJ, et al. Fractionated electrograms in dilated cardiomyopathy: origin and relation to abnormal conduction. *J Am Coll Cardiol* 1996;27:1071–1078.
13. de Bakker JM, van Capelle FJ, Janse MJ, et al. Slow conduction in the infarcted human heart. 'Zigzag' course of activation. *Circulation* 1993; 88:915–926.
14. Haqqani HM, Tschabrunn CM, Tzou WS, et al. Isolated septal substrate for ventricular tachycardia in nonischemic dilated cardiomyopathy: incidence, characterization, and implications. *Heart Rhythm* 2011;8:1169–1176.
15. Tedrow UB, Stevenson WG. Recording and interpreting unipolar electrograms to guide catheter ablation. *Heart Rhythm* 2011;8:791–796.
16. Callans DJ, Ren J-F, Michele J, Marchlinski FE, Dillon SM. Electroanatomic left ventricular mapping in the porcine model of healed anterior myocardial infarction: correlation with intracardiac echocardiography and pathological analysis. *Circulation* 1999;100:1744–1750.
17. Haqqani HM, Kalman JM, Roberts-Thomson KC, et al. Fundamental differences in electrophysiologic and electroanatomic substrate between ischemic cardiomyopathy patients with and without clinical ventricular tachycardia. *J Am Coll Cardiol* 2009;54:166–173.
18. Hussein A, Jimenez A, Ahmad G, et al. Assessment of ventricular tachycardia scar substrate by intracardiac echocardiography. *Pacing Clin Electrophysiol* 2014;37:412–421.
19. Rösner A, Barbosa D, Aarsæther E, Kjørås D, Schirmer H, D'hooge J. The influence of frame rate on two-dimensional speckle-tracking strain measurements: a study on silico-simulated models and images recorded in patients. *Eur Heart J Cardiovasc Imaging* 2015;16:1137–1147.
20. Badano LP, Koliás TJ, Muraru D, et al. Standardization of left atrial, right ventricular, and right atrial deformation imaging using two-dimensional speckle tracking echocardiography: a consensus document of the EACVI/ASE/Industry Task Force to standardize deformation imaging. *Eur Heart J Cardiovasc Imaging* 2018;19:591–600.